Donor−Acceptor Distance and Protein Promoting Vibration Coupling to Hydride Transfer: A Possible Mechanism for Kinetic Control in Isozymes of Human Lactate Dehydrogenase

Jodi E. Basner[†] and Steven D. Schwartz*[,†,‡]

Department of Physiology and Biophysics and Department of Biochemistry, Albert Einstein College of Medicine, 1300 Morris Park Avenue, Bronx, New York 10461

Received: August 14, 2003; In Final Form: October 20, 2003

Theoretically based computational methods have been developed in our group to identify protein motions, symmetrically coupled to the reaction coordinate, which modulate the width and height of the barrier to reaction. Previous studies have applied the methods to horse liver alcohol dehydrogenase (HLADH), to help explain experimental kinetic isotope effects. In this paper the methods have been applied to the two isoforms of human lactate dehydrogense (LDH) enzymes which facilitate hydride transfer during the interconversion of pyruvate and lactate. LDH isoforms have evolved to accommodate substrate demand in different parts of the body. The active sites of the isoforms are identical in amino acid content yet the kinetics are distinct. We have performed molecular dynamics simulations for each isoform with either substrate bound. The signature of the protein promoting vibration (PPV) is distinct for each isoform due to differences in the donor−acceptor distance. We hypothesize that kinetic control of hydride transfer may be exerted via a decreased donor−acceptor distance when lactate is bound to the heart isoform and when pyruvate is bound to the skeletal muscle isoform. The identity, frequency, and position of active site amino acid motions correlated to the donor−acceptor motion also vary for each isoform. These results demonstrate that even in almost identical enzymes, subtle differences in protein structure, remote from the active site, can have significant effects on reaction dynamics.

Introduction

Directed dynamical influences on enzymatic catalysis, via internal protein motions, have begun to be investigated through theoretical, computational, and experimental techniques.[1−12] Historical paradigms of catalysis, such as transition state stabilization and ground-state destabilization, provide static "snapshots" of reaction coordinate evolution. In the work reported in this paper we study two isozymes of human lactate dehydrogenase. Lactate dehydrogenase (LDH) catalyzes the interconversion of the hydroxy-acid lactate and the keto-acid pyruvate with the coenzyme nicotinamide adenine dinucleotide (Figure 1).[13] This enzyme plays a fundamental role in respiration, and multiple isozymes have evolved to enable efficient production of substrate appropriate for the microenvironment.[14] Two main subunits, referred to as heart and muscle (skeletal), are combined in the functional enzyme as a tetramer to accommodate aerobic and anaerobic environments. Subunit combinations range from pure heart (H_4) to pure muscle (M_4). The reaction catalyzed involves the transfer of a proton between an active site histidine and the C2 bound substrate oxygen, as well as hydride transfer between C4N of the cofactor, NAD(H), and C2 of the substrate (Figure 1). Remarkably, the domain structure, subunit association, and amino acid content of the human isozyme active sites are comparable, but their kinetic properties are distinct. Read et al.[17] have reported the influence of surface electrostatic effects peripheral to the active site on the pK_a of the active site histidine. The charge differences of each isozyme's peripheral amino acids lead to a variation of

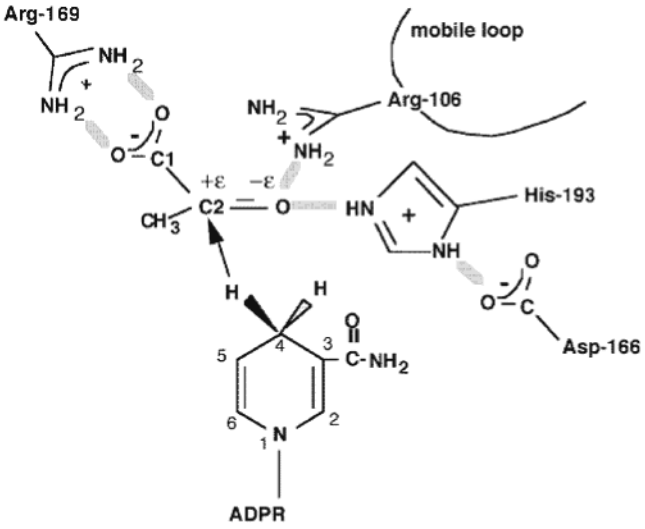

Figure 1. Diagram of the binding site of LDH with bound NADH and pyruvate showing hydrogen bonds between the substrate and key catalytically important residues of the protein. The catalytic event involves the hydride transfer of the C4 hydrogen of NADH from the pro-R side of the reduced nicotinamide ring to the C2 carbon of pyruvate and protein transfer from the imidozole group of His-193 to pyruvate's keto oxygen. Adapted from ref 11.

0.96 in the pK_a, with M the lower of the two. Since pyruvate cannot bind to the active site unless the histidine is protonated, these results are consistent with the redox environment of each isoform and reported K_M value. To note, pyruvate inhibition, where pyruvate forms a covalent complex with NAD^+, is thought to contribute to the decreased rate of pyruvate turnover in the H isoform, but the rates reported here were determined

* Corresponding author. E-mail: sschwartz@aecom.yu.edu.
† Department of Physiology and Biophysics.
‡ Department of Biochemistry.

10.1021/jp0364349 CCC: $27.50
Published on Web 12/04/2003

before the onset of inhibition. The rate term k_{cat}, defined as moles substrate consumed per mole active site per second, is approximately twice as fast for lactate production in the M isoform than in the H isoform. These authors also demonstrate the minor effects of pH changes on k_{cat}. Their analysis highlights the kinetic differences due to substrate binding. Differences are also possible in other stages of this sequential reaction, including cofactor binding, loop closure, chemical reaction, cofactor release, substrate release, and loop opening. This work proposes a mechanism whereby placement of the transition state, coupled with a promoting vibration, can influence kinetic control of hydride transfer.

Developments in our group have focused on theoretically derived computational methods that identify specific protein motions, symmetrically coupled to the reaction coordinate, that affect the efficiency of enzyme catalysis.[18] Dubbed protein-promoting vibrations (PPV), these motions modulate the width and height of the reaction barrier and have been used to explain experimental results involving hydride tunneling. The large mass of a hydride, compared to an electron, and the dependency of the probability of tunneling on transfer distance cause hydride transfer reactions to be particularly sensitive to these barrier modulations. The pattern of kinetic isotope effects (KIE) in the alcohol dehydrogenase from thermophilic *Bacillus stearothermophilus* (ADH-ht) have been rationalized with a model that includes a PPV.[3,19,20] At and below room temperature, tunneling decreases in ADH-ht, contrary to predictions for tunneling through a rigid barrier. From 30 to 60 °C, tunneling increases and the KIE is small and temperature independent (compared to a strong dependence at lower temperatures). These results all defy expectations based upon transition state theory and suggested the influence of PPV at higher temperatures for ADH-ht. Protein rigidity at lower temperatures attenuates dynamic influences. Molecular simulations of horse liver alcohol dehydrogenase (HLADH) have indicated the presence of a PPV at 125 cm^{-1}.[20] Additionally, both experiments and molecular dynamics simulations have identified active site amino acids in HLADH that influence transfer distance by directed, bulk dependent, motions on the donor and acceptor atoms.[21] For example, Val203, which impinges on the nicotinimide ring of the cofactor NAD(H), forces the ring's reactive carbon (C4) closer to the substrate, facilitating hydride transfer. Another example of such structural changes can be found in the work of Goldstein and Klinman et al. in which they find that mutation of the Val203 to Ala allows the C4 carbon to relax away from the substrate.[22]

It has been demonstrated with a model system that a reaction coordinate, *s*, antisymmetrically coupled to environmental oscillators and symmetrically coupled to an oscillator, *Q*, via the term Cs^2Q, will exhibit reaction coordinate dependent peaks in the spectral density.[18] The spectral density is the force on *s* from the environment weighted by the density of states of the environment oscillators. A peak exists at the effective frequency of *Q* (the PPV) which increases with the reaction coordinate and vanishes when the force of the PPV on the reaction coordinate is zero, leaving only the influence of solvent forces. Referred to as the point of minimal coupling, it is the putative transition state, although not rigorously proven to be so. We will concentrate, as in alcohol dehydrogenase, on the donor−acceptor motion as a candidate for a PPV. Further details of the analysis are presented in the Molecular Dynamics Simulation section.

Confirmation of the existence of a PPV in both isozymes of LDH will be presented. Distinctions in the nature of each isozyme coupling of the PPV to hydride transfer through variations in donor−acceptor distance and active site motions will be discussed. Active site amino acids within 10 Å of the donor and acceptor are identified as potential targets for mutagenesis due to their strong, directed correlation to the donor−acceptor motion. One simulation demonstrating the effects of mutagenesis will also be presented.

Methods

Molecular Dynamics Simulation. Crystal structures for homotetrameric human heart, h-H_4LDH, and muscle, h-M_4LDH, isozymes in a ternary complex with NADH and oxamate were solved by Read et al.[17] at 2.1 and 2.3 Å resolution, respectively (Brookhaven PDB ID: H_4-1I0Z, M_4-1I10). CHARMM[23] (MSI, San Diego, Ca) molecular dynamics simulations were performed on a Silicon Graphics workstation using the CHARMM27, all hydrogen force field, which includes specific parameters for NAD^+/NADH.[24] Oxamate (NH_2COCOO), an inhibitor of LDH, is an isosteric, isoelectronic mimic of pyruvate with similar binding kinetics.[11] Changes to the PDB files to accommodate reactant and product structures included replacement of the oxamate nitrogen with carbon to create pyruvate/lactate, replacement of the active site neutral histidine to a protonated histidine for the simulation involving pyruvate (residue number 193 or 192, in the heart or muscle isoform, respectively), and removal of the hydride from lactate to NAD^+ to create NADH for the pyruvate simulation. Protein structure (PSF) and coordinate (CRD) input files were created using Insight2000.1 (MSI, San Diego, Ca). Crystallographic waters were treated as TIP3P residues.[25] Two subunits per enzyme were used in all molecular dynamics simulations.

Minimization, dynamics, and analysis followed previous procedure.[20] Each configuration was minimized for 1000 steps using steepest descent with a force criterion of 0.001 kcal per 10 steps and then for 8000 steps using an adopted-basis Newton−Raphson algorithm. The equations of motion were solved using Leapfrog Verlet integration with time step 1 fs. The dynamics protocol consisted of heating for 2 ps during which the temperature was raised to 300 K at a rate of 3 K every 20 integration steps, equilibration for 10 ps, and 30 ps of observation in which 6000 coordinate structures and velocities were recorded. During dynamics, all bonds between a heavy atom and hydrogen, as well as substrate bonds, were constrained with SHAKE.[25] Insight2000.1 uses an atom's chemical environment for potential type assignment in the case of an unparameterized component. Although the assignment proved reliable for lactate, some complications occurred with pyruvate. Insight's assignment caused an immediate break in the C2−C1 carbon bond upon minimization. From the atom types available in the CHARMM27 topology file, the C2 carbon was assigned a carbonyl type (20) and the C1 also a carbonyl type, but it more closely resembles a carboxylate ion such as for a charged C-terminus (32). The bond still requiring an artificial constraint was held by SHAKE[25] throughout the MD simulation. Future analysis will include specific parameterization of the substrates.

The reaction coordinate is defined as follows:

$$s = [R_H - (m_D R_D + m_A R_A)/(m_D + m_A)]\cdot\hat{r}_{DA}$$

where m_i,R_i (i = D, A, H) denote masses and position vectors, of the donor, acceptor, and hydride, respectively, and $\hat{r}_{DA}$ is the unit vector along the donor−acceptor axis. Velocity autocorrelation functions for the donor−acceptor relative motion and reaction coordinate, each projected onto the donor−acceptor

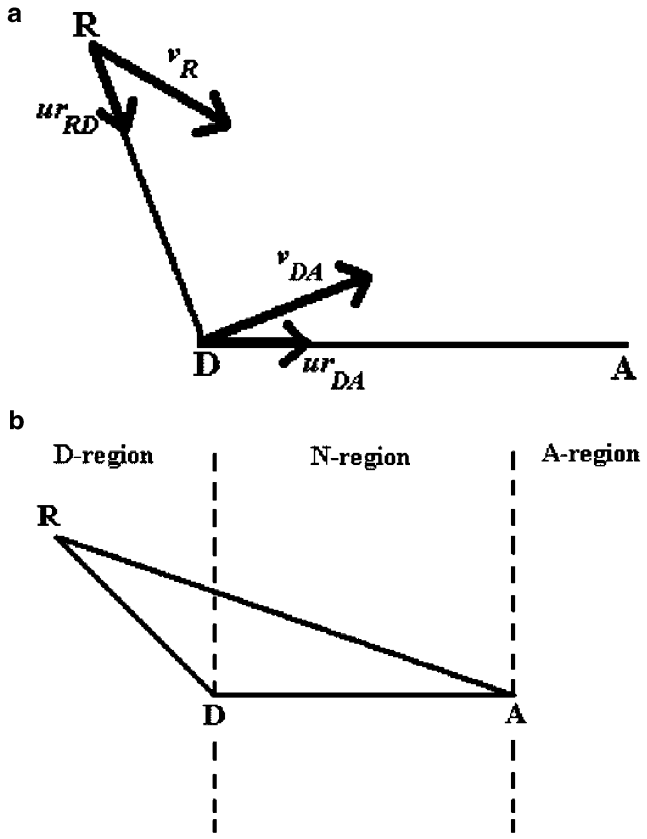

Figure 2. (a) Motions of interest: R = residue center of mass; D = donor; A = acceptor. Vectors are defined in the text. Adapted from ref 21. (b) Angles RDA and RAD, measured to determine where the residue is in space in relation to donor and acceptor: R = residue center of mass; D = donor; A = acceptor. Adapted from ref 21.

axis, were Fourier transformed and then smoothed with the Savitzky−Golay[26] method. As stated previously,[20] the reason for using velocity versus force time series is to eliminate interference of high-frequency protein modes with the low-frequency modes of interest.

Identification of Correlated Active Site Residues.[21] An algorithm developed in our group identifies amino acids whose motion is both correlated with the donor−acceptor motion at the dominant PPV frequency and directed toward the donor (D region) or acceptor (A region). Another possibility is that the amino acid (N region) is located at angles between donor and acceptor and therefore may disrupt rather than force the donor and acceptor closer together (Figure 2b). If the angle formed by the amino acid, the acceptor, and the donor is greater than 90°, then the amino acid is located on the acceptor side (A region). Similar logic follows for the D region, and if both angles are less than 90° the amino acid is in the N region. This division of regions is an important filter to recognize the potential influence of the amino acids on donor−acceptor motion; however, the amino acids along the region boundaries and in the N region must be examined more closely to determine whether they enhance or disrupt donor−acceptor motion. Details of the algorithm are reported elsewhere.[21] Briefly, to determine the correlation of an amino acid's motion with donor−acceptor motion we computed two vector projections (Figure 2a):

$$A(t) = \vec{v}_{\mathrm{DA}} \cdot \vec{ur}_{\mathrm{DA}}$$

$$B(t) = (\vec{v}_{\mathrm{R}} \cdot \vec{ur}_{\mathrm{RD}})(\vec{ur}_{\mathrm{RD}} \cdot \vec{ur}_{\mathrm{DA}})$$

Here, $A(t)$ is the donor−acceptor relative velocity projected on the donor−acceptor axis and $B(t)$ is the velocity of the center of mass of the amino acid (R) projected on the donor (or acceptor) times the component of this motion in the direction of the donor−acceptor axis.

The time-correlation function of these two quantities is then computed with a time average assumed equivalent to the ensemble average via an ergodic hypothesis:

$$C_{\mathrm{AB}}(\tau) = \lim_{T\to\infty} \frac{1}{2T} \int_{-T}^{T} A(t+\tau)\mathrm{B}(t)\, \mathrm{d}t$$

When Fourier transformed, the strength of peaks near the frequency of the PPV is an indicator of a residues ability to be part of the PPV.

Mutagenesis. Using Insight2000.1, Valine 31 in both subunits of lactate bound heart-LDH was replaced with Alanine (V31A). This substitution does not change charge since both are hydrophobic nonpolar amino acids, but does change size since Alanine is smaller by a [$-CHCH_3$] group. Molecular dynamics and data analysis followed the above procedures.

Results and Discussion

Identification of a PPV. Results will be presented for the following six configurations: the heart and muscle isoform each with lactate and NAD^+ bound, the heart and muscle isoform each with pyruvate and NADH bound, and two simulations of the heart isoform with lactate and NAD^+ bound where the hydride distance was definitively restrained at a point between donor and acceptor carbons. For each configuration, reaction coordinates and donor−acceptor spectra from a 30 ps simulation will be discussed. To identify the presence of a PPV there should be near overlap between peaks in a pair of corresponding reaction coordinate and donor−acceptor spectra. In Figure 3a, the heart-LDH lactate donor−acceptor spectrum, there is a pronounced peak at approximately 270 cm^{-1}. The reaction coordinate spectrum's pattern of peaks closely resembles its donor−acceptor pair in the dominant frequency region with a strong peak about 250 cm^{-1} (Figure 3b). The dominant peak of the heart-LDH pyruvate spectra appears at a lower frequency than lactate, occurring at approximately 130 cm^{-1} as seen in Figure 3. The donor−acceptor relative motion is likely to be anharmonic in complex systems such as enzymes. The larger amplitude peak reflects that a greater portion of the motion is at that frequency. Typically, the donor−acceptor and reaction coordinate spectra coincide in which peak is of greater amplitude. This is not true, however, for the spectra of muscle-LDH with lactate bound, where the peak amplitudes in the donor−acceptor spectrum are nearly equal and for the reaction coordinate spectrum the higher frequency peak is clearly dominant (Figure 4). We will discuss other features that reinforce the identity of these lower modes as the PPV. Overlapping dominant peaks in the donor−acceptor and reaction coordinate spectra are a strong indication that the donor−acceptor motion is strongly coupled to the reaction coordinate.

To determine if the donor−acceptor motion is symmetrically coupled to the reaction coordinate (s), the hydride is held at a fixed distance from the donor and acceptor throughout the simulation. With fixed s the reaction coordinate spectrum is a superposition of two forces, namely from thermal motions of the protein and from the PPV. In this model the spatial dependence of the force on s is caused only by the PPV. For simplicity, we can imagine a double-well 2D barrier potential; at the point of minimal coupling, where s equals zero, the particle is at the top of the barrier to reaction and will not

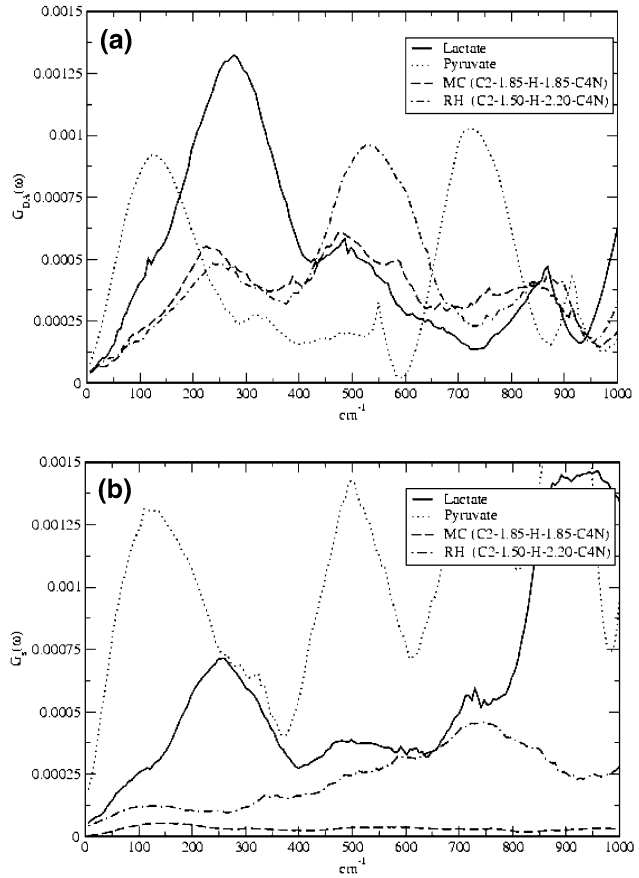

Figure 3. (a) Spectral density $G_{DA}(\omega)$ for the donor−acceptor relative motion in the wild-type human heart lactate dehydrogense isoform; it monitors the relative motion between the substrate C2 carbon and carbon C4N of the nicotinimide ring of the cofactor NAD^+/NADH. The solid line represents the configuration where lactate and NAD^+ are bound, the dotted line is where pyruvate and NADH are bound, the dashed line is the minimal coupling (MC) simulation with lactate and NAD^+ bound and the (hydride-C2) and (hydride-C4N) distances restrained, and the dot−dash line is exemplary of the restrained hydride (RH) simulations to search for the point of minimal coupling. Distances are in Angstroms and defined in the form (C2-Å−Hydride-Å−C4N). The power spectrum is reported in CHARMM units. (b) The spectral density $G_s(\omega)$ for the reaction coordinate in the wild-type human heart lactate dehydrogense isoform. The solid line represents the configuration where lactate and NAD^+ are bound, the dotted line is where pyruvate and NADH are bound, the dashed line is the minimal coupling (MC) simulation with lactate and NAD^+ bound and the (hydride-C2) and (hydride-C4N) distances restrained, and the dot−dash line is exemplary of the restrained hydride (RH) simulations to search for the point of minimal coupling. Distances are in Angstroms and defined in the form (C2-Å−Hydride-Å−C4N). The power spectrum is reported in CHARMM units.

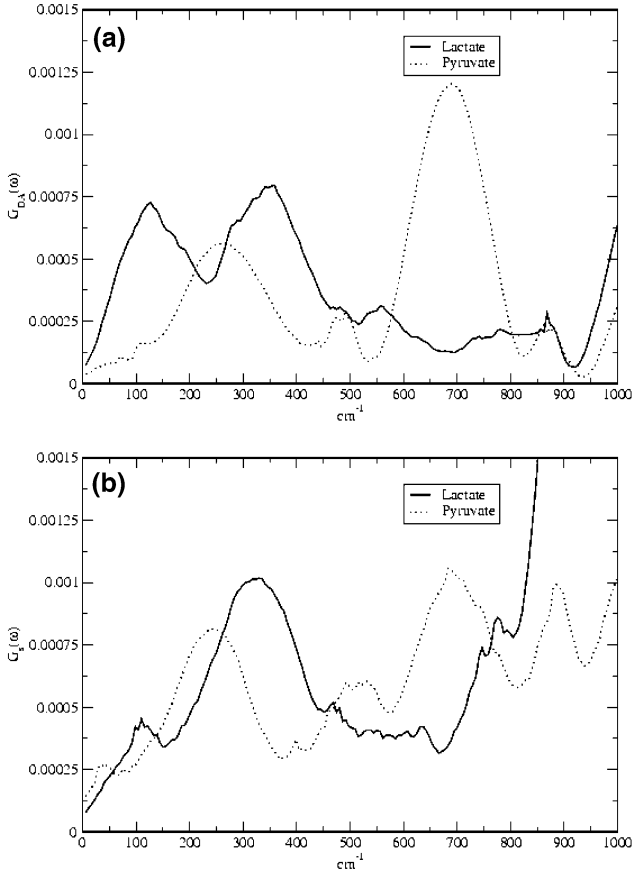

Figure 4. (a) The spectral density $G_{DA}(\omega)$ for the donor−acceptor relative motion in the wild-type human muscle lactate dehydrogense isoform; it monitors the relative motion between the substrate C2 carbon and carbon C4N of the nicotinimide ring of the cofactor NAD^+/NADH. The solid line represents the configuration where lactate and NAD^+ are bound, and the dotted line is where pyruvate and NADH are bound. The power spectrum is reported in CHARMM units. (b) The spectral density $G_s(\omega)$ for the reaction coordinate in the wild-type human muscle lactate dehydrogense isoform. The solid line represents the configuration where lactate and NAD^+ are bound, and the dotted line is where pyruvate and NADH are bound. The power spectrum is reported in CHARMM units.

experience any forces from the PPV. The force, due to the donor−acceptor motion, on the reaction coordinate will increase as *s* increases (this holds true as long as there is a quadratic expansion of the potential as in the model). Two simulations, where the hydride is constrained with the intention of locating the point of minimal coupling, for the lactate-to-pyruvate reaction direction are shown in Figure 3. The most reduced reaction coordinate spectrum, equidistant from donor and acceptor at 1.85 A, is the point of minimal coupling (Figure 3b). The other simulation is exemplary as the reaction coordinate peak increases with hydride displacement from the point of minimal coupling.

Using a quadratic expansion for the PPV potential, it can be shown that the amplitude of the reaction coordinate peak is also proportional to donor−acceptor distance. As explained above, in the simulations where the hydride is restrained, the reaction coordinate peak increases when *s* increases. The amplitude of the peak in the reaction coordinate spectra will reflect the size of *s*, or the distance from the point of minimal coupling to the donor or acceptor. Naturally the donor−acceptor distance will determine the maximum displacement from the point of minimal coupling and the overall degree of the PPV coupling (in our model the strength is assumed constant as a function of distance). Comparisons of donor−acceptor distance are appropriate within an isozyme, where it is thought that other factors determining peak amplitude will be of equal magnitude. The donor−acceptor distance was recorded over the 30 ps simulation. Comparing Figure 5 with the reaction coordinate spectrum for heart-LDH (Figure 3b), the greater donor−acceptor distance for pyruvate is reflected in the spectra as a greater amplitude peak. Figure 6 illustrates this comparison for muscle-LDH where lactate has the greater donor−acceptor distance of the two substrates. The results here highlight the intuitive influence of the donor−acceptor distance on the PPV. It is also reasonable to consider its influence on the reaction rates. It may be that hydride transfer is a critical step in the isozyme's substrate control. To create these properties, nature has facilitated hydride transfer via

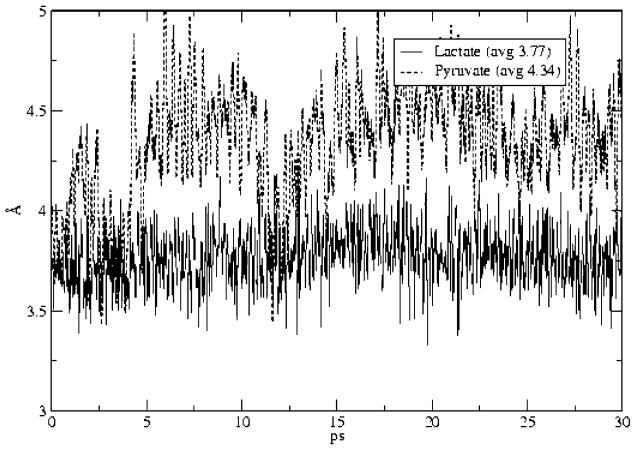

Figure 5. Donor−acceptor distance for the wild-type human heart lactate dehydrogenase isoform; this is the distance between the C2 carbon of substrate and carbon C4N of the nicotinimide ring of the cofactor NAD^+/NADH. The solid line represents the configuration where lactate and NAD^+ are bound, and the dashed line is where pyruvate and NADH are bound.

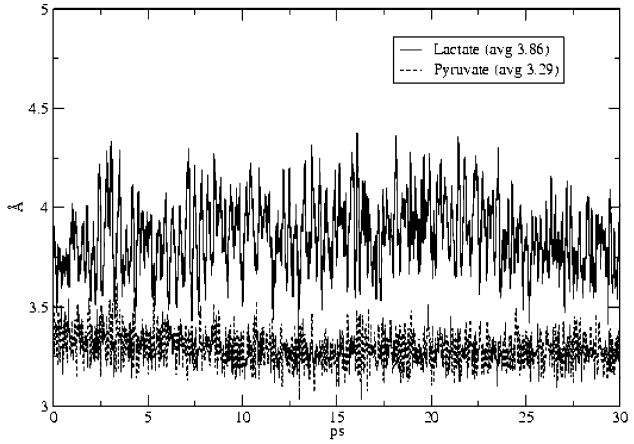

Figure 6. Donor−acceptor distance for the wild-type human muscle lactate dehydrogenase isoform; this is the distance between the C2 carbon of substrate and carbon C4N of the nicotinimide ring of the cofactor NAD^+/NADH. The solid line represents the configuration where lactate and NAD^+ are bound, and the dashed line is where pyruvate and NADH are bound.

decreased donor−acceptor distance. From a slightly different perspective we can imagine, for example, that when lactate is bound in heart-LDH while the hydride is transferred to the cofactor NAD^+, the process of creating pyruvate, the donor−acceptor distance increases. Therefore, the distance from the hydride's position now at NADH to $s = 0$ will be larger, and this will be reflected as a larger peak in the reaction coordinate spectral density.

Identification of PPV Correlated Active Site Residues. Approximately 60 amino acids were identified to be within 10 Å (an arbitrary cutoff) of the donor and acceptor in each isozyme. To determine which are strongly correlated to the donor−acceptor motion, the residues were ordered by their greatest amplitude peak within range of their respective dominant peak in the donor−acceptor spectrum. Since the dominant peaks of the donor−acceptor spectra are broad, a range was used to determine resonant motions. For example, for the heart-LDH, lactate bound, configuration, the residue spectra were scanned between 175 and 315 cm^{-1}. Table 1 lists the top 15 amino acids of each isozyme−substrate configuration along

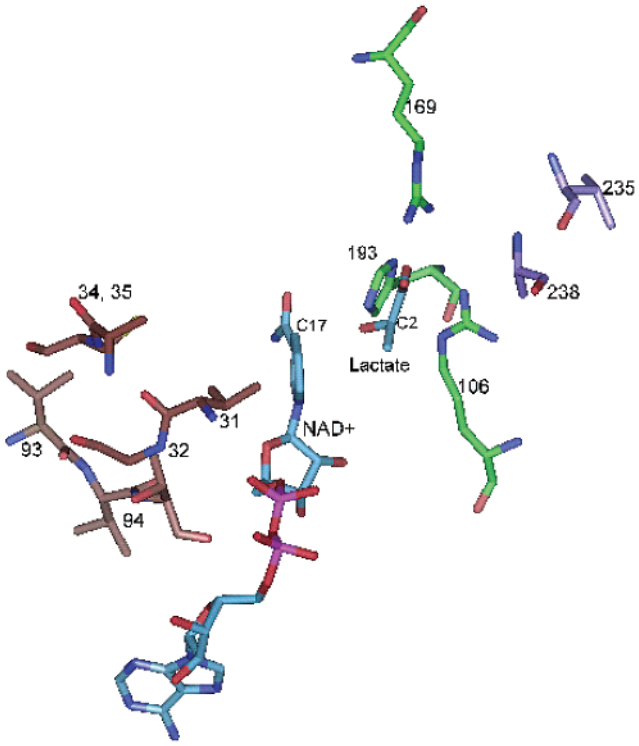

Figure 7. From the final structure of the heart isoform with lactate and NAD^+ bound. The blue bonded molecules are lactate and NAD^+. The purple bonded are behind lactate (D region) and are strongly correlated with the donor−acceptor motion, namely the relative motion of the substrate C2 carbon and carbon C4N of the nicotinimide ring of the cofactor NAD^+. The brown bonded are behind NAD^+ (A region) and are strongly correlated with the donor−acceptor motion. The green bonded are landmark and/or weakly correlated residues as described in the text.

with the frequency at which their spectrum has greatest amplitude. The bold residues are conserved within an isozyme independent of which substrate is bound, and the italic residues are conserved across all four configurations. Although the majority of residues are the same across configurations, a closer look will show that the same residue has maximal resonance with the donor−acceptor motion at varied frequency, magnitude, and position. Angles were measured in the final structure of the 30 ps simulation according to Figure 2b. The amplitude is the portion of residue motion both directed toward donor/acceptor and along the donor−acceptor axis; the residues will vibrate at other frequencies and in other directions which presumably combinations of will reveal other cooperative influences. The amplitude has been multiplied by 10^5 for convenience. Figure 7 highlights some of the important residues in the heart-LDH configuration with lactate bound. The essential active site histidine 193 is included as a landmark and as an example of a poorly correlated residue (Figure 8). It is reasonable that histidine 193 would be weakly correlated. Although it needs to be directed toward the substrate, it should not be pushing so hard that the substrate is pushed away. Other analysis showed that a significant portion of its motion is directed parallel to the donor−acceptor axis. Arginine 169, another chemically important residue that stabilizes the substrate by solvating the charged carboxylic moiety, is also shown for orientation. The variation in correlation strength of active site amino acids stresses the importance of incorporating dynamics into theories of enzyme catalysis. Arginine 106 has been included in Figure 7 to reinforce this point. Although in the static picture it appears to be ideally situated to push the donor

TABLE 1: The 15 Active Site Amino Acids Most Strongly Correlated with Donor−Acceptor Motion[a]

Lactate Bound LDH: Donor = Lactate, Acceptor = NAD+						Pyruvate Bound LDH: Donor = NADH, Acceptor = Pyruvate					
		angle						angle			
heart,lactate	A. A.	RAD	RDA	ν (cm^{-1})	Amp.$\times 10^5$	heart,pyruvate	A. A.	RDA	RAD	ν (cm^{-1})	Amp.$\times 10^5$
240D	E	39	130	271	9.1	***237A***	S	33	127	98	11.3
94A	V	135	33	173	9.3	***235A***	V	28	139	93	11.5
136A	V	129	30	196	9.4	104A	E	42	121	93	11.7
194D	G	27	139	271	9.4	135D	V	125	39	104	12.0
235D	V	18	154	173	9.7	**94D**	V	142	27	133	13.0
31A	V	138	25	283	10.4	***236A***	E	19	154	110	13.4
256A	V	139	29	271	10.4	**136D**	V	132	28	75	13.5
236D	E	20	153	179	10.6	***238A***	A	15	153	139	14.1
95A	T	137	30	173	10.8	***95D***	T	139	27	93	14.1
35A	C	167	9	173	12.8	***34D***	A	139	29	127	14.1
34A	A	145	25	185	13.2	239A	Y	10	164	93	14.4
32A	G	150	21	266	13.2	***35D***	C	158	15	145	14.7
93A	V	156	18	173	14.8	**256D**	V	145	24	75	15.0
253A	G	136	30	208	15.8	***32D***	G	145	24	139	16.8
238D	A	22	145	179	16.3	**93D**	V	165	11	104	17.3

muscle,lactate	A. A.	RAD	RDA	ν (cm^{-1})	Amp.$\times 10^5$	muscle,pyruvate	A. A.	RDA	RAD	ν (cm^{-1})	Amp.$\times 10^5$
255A	V	115	51	330	4.5	239D	E	39	131	179	4.5
34A	C	154	18	278	5.0	***34A***	C	154	20	202	4.7
29A	A	131	34	341	6.0	135A	V	131	32	289	4.7
234D	V	13	161	301	6.2	***252A***	G	123	44	248	4.9
236D	S	21	148	278	6.4	***233D***	V	31	140	289	5.1
235D	E	6	172	289	6.5	***94A***	T	157	17	196	5.1
160N	S	101	58	278	6.6	**194D**	D	23	151	277	5.6
194D	D	29	142	376	6.8	***234D***	V	17	158	266	5.9
94A	T	156	16	295	6.8	***235D***	E	2	177	260	6.3
252A	G	108	53	289	6.9	***236D***	S	24	147	254	6.9
33A	A	143	27	359	7.4	**29A**	A	132	36	277	7.3
30A	V	153	16	284	7.5	***193D***	G	26	144	243	7.6
193D	G	35	131	284	12.4	***30A***	V	150	19	260	7.8
237D	A	10	162	278	12.6	***237D***	A	27	140	271	9.9
31A	G	166	10	318	13.1	***31A***	G	165	11	254	10.5

[a] If lactate is bound, NAD^+ is the acceptor. If pyruvate is bound, NADH is the donor. See Figure 2 for angle definitions. Bold amino acids are among the top 15 for an isozyme, independent of substrate bound. Italic amino acids are among the top 15 for both isozymes, independent of substrate bound. The peak amplitude has been multiplied by 10^5 for convenience (Amp $\times 10^5$). Frequency screens: H_2, lactate (175−315 cm^{-1}), H_2,pyruvate (75−315 cm^{-1}), M_2, lactate (175−375 cm^{-1}), M_2, pyruvate (175−375 cm^{-1}). A. A. abbreviates amino acid.

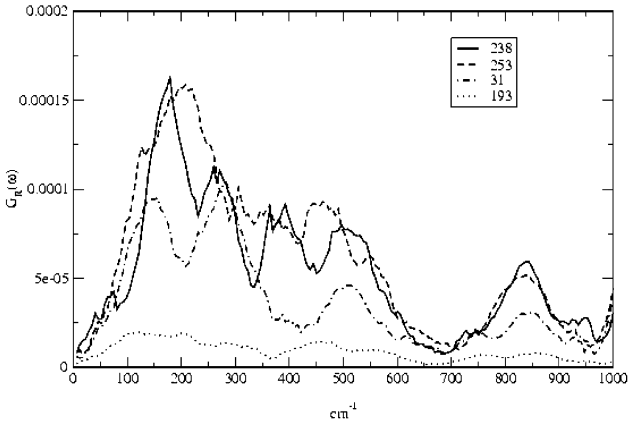

Figure 8. Spectral density $G_R(\omega)$ of four residues in the wild-type human heart lactate dehydrogenase isoform with lactate and NAD^+ bound. Compare with Table 1; residue 238 is the most strongly correlated residue, 31 is strongly correlated and substituted in the mutagenesis simulation, and residue 193, the essential active site histidine, is poorly correlated. The power spectrum is reported in CHARMM units.

toward acceptor, the algorithm shows that it has approximately half the correlation strength of the maximally correlated residue, 238 (Table 1), with an amplitude of 8.5 units.

The identification of the correlated active site residues is a clear guide to select a residue for a mutagenesis study. As mentioned in the Introduction, computational mutagenesis studies in HLADH (horse liver alcohol dehydrogenase) support corresponding experimental results which indicate that a Valine residue that impinges on the reactive carbon of the NAD^+ nicotinimide ring significantly influences the height and width of the barrier potential. As seen in Figure 7 and Table 1, Valine 31, a strongly correlated residue in lactate-bound heart-LDH, parallels the role played by Val 203 in HLADH by impinging on the nicotinimide ring of the NAD^+ cofactor and by being strongly correlated with the PPV. As was done in HLADH, Valine 31 was replaced with the less bulky Alanine residue. Figure 9a is the reaction coordinate spectrum compared with the wild type. The amplitude of the dominant peak has been approximately halved. Above we discussed that the donor−acceptor distance and the coupling of the donor−acceptor motion (coupling strength constant) to the reaction coordinate are proportional to the amplitude of the reaction coordinate spectral density. Changing an active site residue will affect the strength of coupling as compared to the cases described above where the protein remained the same while a reactant was changed. Figure 9b compares the donor−acceptor distance of the mutant with the wild type. The donor−acceptor distance has increased, therefore it must be the case that a significant decrease in the strength of coupling is causing the amplitude reduction in the reaction coordinate peak. Combining these computational methods, identification of a PPV and strongly

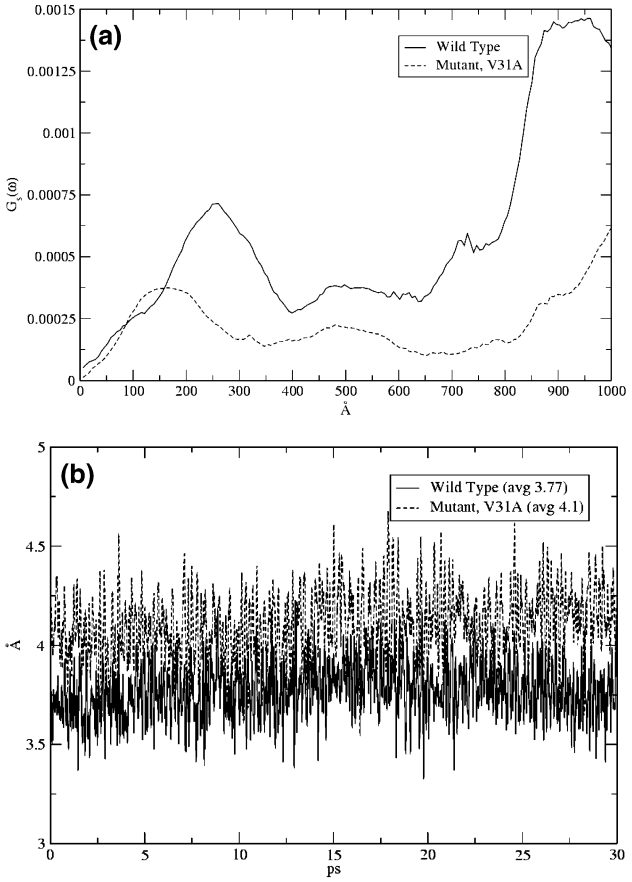

Figure 9. (a) Spectral density $G_s(\omega)$ for the reaction coordinate in the wild type and mutant human heart lactate dehydrogense isoform with lactate and NAD^+ bound. The solid line is the wild-type configuration where residue 31 is Valine, and the dashed line is the mutant configuration where residue 31 is Alanine. The power spectrum is reported in CHARMM units. (b) Donor−acceptor distance for the wild type and mutant human heart lactate dehydrogenase isoform with lactate and NAD^+ bound. The solid line represents the wild-type configuration where residue 31 is Valine and the dashed line represents the mutant configuration where residue 31 is Alanine.

correlated active site amino acids, results in a rational approach to experimental mutagenic studies.

Conclusion

Earlier studies focused on the identification of a protein-promoting vibration in HLADH, as well as active site amino acids that influence the coupling of the promoting vibration to the reaction coordinate. Experimental studies with HLADH indicate that tunneling is a significant contribution to the hydride transfer reaction. Theoretical predictions involving promoting vibrations that modulate barrier height and width reproduced experimental trends that previously were obscure. A key is the modulation of barrier width and the sensitivity of a hydride to transfer distance. The extent of the promotion of vibrational force on the reaction coordinate determines the extent of tunneling and also affects over-the-barrier transfer via modulation of the barrier height. This study demonstrates that the signature of a protein promoting vibration elucidated with the HLADH enzyme is also characteristic of the LDH enzymes. Whether tunneling is part of the transfer kinetics of LDH remains to be seen, but certainly the presence of protein-promoting vibrations indicates the need to include dynamical effects for an accurate calculation of hydride transfer.

The LDH isozymes offer the opportunity of a comparative study. The differential expression of the isozymes in the body has evolved to handle the "unwanted" substrate of the local environment, for example, the heart's inability to tolerate high lactate concentrations and thus the efficiency of the heart isoform to convert lactate to pyruvate. Although the same amino acids comprise the active site, this study has revealed distinct differences in active site motions upon substrate binding. These divergent motions will influence reaction parameters such as the distance from the point of minimal coupling, $s = 0$, to the substrate and in turn affect the efficiency of hydride transfer. Simulations where the hydride is restrained at a definite distance from the donor and acceptor determined that the donor−acceptor motion is symmetrically coupled to the reaction coordinate, a property known to promote reaction rates. As the reaction coordinate is displaced from $s = 0$, the peak increases because of the spatial dependence of the PPV.

The kinetic analysis of the isozymes is not yet complete. Rates have only been measured for one reaction direction, and there are no data available on kinetic isotope effects. We must hesitate to compare across isoforms with pyruvate bound as in the experimental data. The coupling constant from ref 18 is assumed constant within each isoform, i.e., independent of which substrate is bound, but it is incorrect to maintain this assumption across isoforms. This is supported by the sharp degree of change in the coupling constant with a single amino acid mutation. The comparison may also be artificial since the hydride transfer step is not rate-limiting. However, the motivation of the experimental study was due to the extreme overlap of the isoform properties, including the identity of the active site amino acids, the identity and conformation of the amino acids of the specificity loop, large scale geometries, and the near similarity of the cofactor K_D values. The experiments revealed that changes in the pH had major effects on the binding ability of pyruvate and minor effects on the k_{cat}; does this exclude variations in substrate binding and perhaps loop activity from contributing to the differences in k_{cat}? It is interesting to consider, supported by the distinctions revealed in this paper, whether hydride transfer may be a significant step of kinetic control of product formation in the LDH isoforms.

In the future, these algorithms coordinated with others will be applied to QM/MM models to further investigate the details of reaction coordinate evolution and transition state structure. With the aid of theoretical models, picosecond motions that influence millisecond biochemical reactions have begun to be characterized.

Acknowledgment. We gratefully acknowledge the support of the Office of Naval Research and the National Science Foundation through grants CHE-9972864 and CHE-0139752. J.E.B. additionally thanks Dimitri Antoniou and Joshua Mincer for helpful conversations.

References and Notes

(1) Hur, S.; Bruice, T. C. *J. Am. Chem. Soc.* **2003**, *125*, 1472−1473.
(2) Antonious, D.; Caratzoulas, S.; Kalyanaraman, C.; Mincer, J. S.; Schwartz, S. D. *Eur. J. Biochem.* **2002**, *269*, 3103−3112.
(3) Antoniou, D.; Schwartz, S. D. *J. Phys. Chem. B* **2001**, *105*, 5553−5558.
(4) Hammes-Schiffer, S. *Biochemistry* **2002**, *41*, 13335−13343.
(5) Ravi Rajagopalan, P. T.; Lutz, S.; Benkovic, S. J. *Biochemistry* **2002**, *41*, 12618−12628.
(6) Luo, J.; Bruice, T. C. *PNAS* **2002**, *99*, 16597−16600.
(7) Bruice, T. C.; Benkovic, S. J. *Biochemistry* **2000**, *39*, 6267−6274.
(8) Basran, J.; Sutcliffe, M. J.; Scrutton, N. S. *Biochemistry* **1999**, *38*, 3218−3222.
(9) Kohen, A.; Klinman, *J. P. Acc. Chem. Res.* **1998**, *31*, 397−404.
(10) Cui, Q.; Karplus, M. *J. Phys. Chem. B* **2002**, *106*, 7927−7947.
(11) Ranganathan, S.; Gready, J. E. *J. Phys. Chem. B* **1997**, *101*, 5614−5618.

(12) Turner, A. J.; Moliner, V.; Williams, I. H. *PCCP* **1999**, *1*(6), 1323−1331.
(13) Gulotta, M.; Deng H.; Deng, H.; Dyer, R. B.; Callender, R. H. *Biochemistry* **2002**, *41*, 3353−3363.
(14) Meister, A. *Advances in Enzymology: And Related Areas of Molecular Biology*; John Wiley & Sons: New York, 1973; Vol. 37.
(15) Hewitt, C. O.; Eszes, C. M.; Sessions, R. B.; Moreton, K. M.; Dafforn, T. R.; Takei, J.; Dempsey, C. E.; Clarke, A. R.; Holbrook, J. J. *Protein Eng.* **1999**, *12*(6), 491−496.
(16) Eszes, C. M.; Sessions, R. B.; Clarke, A. R.; Moreton, K. M.; Holbrook, J. J. *FEBS Lett.* **1996**, *399*, 193−197.
(17) Read, J. A.; Winter, V. J.; Eszes, C. M.; Sessions, R. B.; Brady, R. L. *Proteins: Struct., Funct., Genet.* **2001**, *43*, 175−185.
(18) Caratzoulas, S.; Schwartz, S. D. *J. Chem. Phys.* **2001**, *114*(7), 2910−2918.
(19) Kohen, A.; Cannio, R.; Bartolucci, S.; Klinman, J. *Nature* **1999**, *399*, 496−499.
(20) Caratzoulas, S.; Mincer, J. S.; Schwartz, S. D. *J. Am. Chem. Soc.* **2002**, *124*(13), 3270−3276.
(21) Mincer, J. S.; Schwartz, S. D. *J. Phys. Chem. B* **2003**, *107*(1), 366−371.
(22) (22) Bahnson, B. J.; Colby, T. D.; Chin, J. K.; Goldstein, B. M.; Klinman, J. P. *Proc. Natl. Acad. Sci. U.S.A.* **1997**, *94*, 12797−12802.
(23) Brooks, B. R.; Bruccoleri, R. E.; Olafson, B. D.; States, D. J.; Swaminathan, S.; Karplus, M. *J. Comput. Chem.* **1983**, *4*, 187−217.
(24) Gao, J.; Pavelites, J. J.; Bash, P. A.; Mackerell, A. D., Jr. *J. Comput. Chem.* **1997**, *18*(2), 221−239.
(25) Jorgensen, W. L.; Chandrasekhar, J.; Madura, J. D. *J. Chem. Phys.* **1983**, *79*, 926−935.
(26) Allen, M. P.; Tildesley, D. J. *Computer Simulation of Liquids*; Clarendon: Oxford, 1987.
(27) Press, W. H.; Flannery, B. P.; Teukolsky, S. A.; Vetterling, W. T. *Numerical Recipes in FORTRAN*, 2nd ed.; Cambridge University Press: Cambridge, 1992.